



Article

Multi-Omics Analysis to Visualize Ecotype-Specific Heterogeneity of the Metabolites in the Mesocarp Tissue of Three Avocado (*Persea Americana* Mill.) Ecotypes

Yu Ge ^{*}, Xiaoping Zang, Yuanzheng Liu, Lixia Wang, Jiashui Wang, Yanxia Li and Weihong Ma ^{*}

Haikou Experimental Station, Chinese Academy of Tropical Agricultural Sciences, Haikou 570102, China; zangxiaoping@catas.cn (X.Z.); liuyuanzheng@catas.cn (Y.L.); wlxmm@163.com (L.W.); wangjiashui@catas.cn (J.W.); liyanxia@catas.cn (Y.L.)

^{*} Correspondence: geyu@catas.cn (Y.G.); zjwhma@catas.cn (W.M.);
Tel.: +86-898-6678-1349 (Y.G.); +86-898-6652-8651 (W.M.)

Abstract: The huge amount of metabolites in avocado mesocarp influences the commercial production of specific avocado fruits for consumption and for industrial applications. Additionally, the diversity in the metabolite content may be used as biomarker for differentiating among various avocado ecotypes. However, the differences in metabolites in avocado remain unclear among various avocado ecotypes. In this study, we first compared the lipid droplets, fatty acid compositions, and gene expression profiles of the mature avocado mesocarps of three ecotypes, and confirmed the differences in the mesocarp oil contents. Furthermore, the lipidomics and metabolomics based on the ultra-high-performance liquid chromatography-triple and time-of-flight mass spectrometry and ultra-high performance liquid chromatography-Q exactive-mass spectrometry were completed, respectively, which revealed considerable differences in the relative amounts of lipids from 10 classes and other metabolites from seven super-classes among the examined avocado ecotypes. The profiles of 65 lipids and 15 other metabolites could be potential candidate biomarkers useful for identifying diverse avocado ecotypes. This is the first comprehensive metabolomics-based comparative investigation of lipid and other metabolites among three avocado ecotypes.

Keywords: avocado; ecotype; fatty acids; lipidomics; metabolomics



Citation: Ge, Y.; Zang, X.; Liu, Y.; Wang, L.; Wang, J.; Li, Y.; Ma, W. Multi-Omics Analysis to Visualize Ecotype-Specific Heterogeneity of the Metabolites in the Mesocarp Tissue of Three Avocado (*Persea Americana* Mill.) Ecotypes. *Horticulturae* **2021**, *7*, 94. <https://doi.org/10.3390/horticulturae7050094>

Academic Editor: Valentina Schmitzer

Received: 1 April 2021

Accepted: 21 April 2021

Published: 1 May 2021

Publisher's Note: MDPI stays neutral with regard to jurisdictional claims in published maps and institutional affiliations.



Copyright: © 2021 by the authors. Licensee MDPI, Basel, Switzerland. This article is an open access article distributed under the terms and conditions of the Creative Commons Attribution (CC BY) license (<https://creativecommons.org/licenses/by/4.0/>).

1. Introduction

Avocado (*Persea americana* Mill.) is one of the most economically important subtropical and tropical fruit crops worldwide, and its production and consumption levels have increased dramatically during the last 150 years [1,2]. Avocado is a highly variable species, with regional variations resulting in diverse ecological races or varieties [3]. The following three avocado ecotypes are widely recognized by horticulturalists: Mexican race (*P. americana* var. *drymifolia*), Guatemalan race (*P. americana* var. *guatemalensis*), and West Indian race (*P. americana* var. *americana*) [4]. These ecotypes are distinguishable based on morphological, horticultural, and physiological traits [3,5]. The Mexican race avocado fruit often contains a relatively high oil content, but is rarely associated with a desirable flavor. The Guatemalan race avocado fruit usually has a moderate amount of oil, with an attractive, creamy or pale-to-buttery yellow pulp and a rich and nutty flavor. In contrast, the West Indian avocado fruit is renowned for its relatively low oil content, as well as a distinctly less nutty flavor [3]. Therefore, the oil content and other metabolites could be the important factors for differentiating among these three avocado ecotypes.

Avocado mesocarp oil is a crucial taste component that is also a key factor influencing fruit quality and nutritional value [6]. Therefore, horticulturalists have studied the oil content of the edible parts of avocado fruit, which affects the market quality of avocado fruit and any derived food products [7,8]. The avocado fruit has also been extensively

investigated regarding its other chemical compositions [9,10]. Natural antioxidants, especially flavonoids and other polyphenols, are potentially useful for the pharmaceutical and food industries because of their many beneficial effects [11]. The avocado fruit contains more phenolic compounds than other kinds of tropical fruits [11–13].

Metabolomics refers to research exploring the dynamic changes to metabolites. An earlier investigation clarified the accumulation patterns and genetic origins of plant metabolites [14]. Metabolomics-based research techniques enable the simultaneous quantification of hundreds of known metabolites and nearly 1000 known and unknown metabolites [15–17]. Especially, lipids are considered to be essential subcellular components of plant fruits, and the MS-based untargeted lipidomics methodology could analyze lipid metabolites including glycerolipids, glycerophospholipids, sterol lipids, and so on [18,19]. Consequently, metabolites can be identified and the relevant metabolic processes may be elucidated.

In this study, we visualized the lipid droplets, analyzed the fatty acid compositions via gas chromatography–mass spectrometry (GC-MS), investigated the lipid-related genes participating in the fatty acid (FA) synthesis and triacylglycerol (TAG) storage in the mature avocado mesocarps of three ecotypes, and elucidated the mesocarp oil content differences among three avocado ecotypes. Then, we analyzed the lipid and other metabolites in the mesocarps of three avocado ecotypes via ultra-high-performance liquid chromatography–triple and time-of-flight mass spectrometry (UHPLC-Q-TOF-MS) and ultra-high performance liquid chromatography-Q Exactive-mass spectrometry (UHPLC-QE-MS), respectively, and then the critical analysis was also done to examine the differences among three avocado ecotypes by classifying lipid and other metabolites according to its classes. This study aims to not only expand food composition data for avocado, but also to facilitate the understanding of biochemical characterization among three avocado ecotypes. The results of this study also offer some metabolites for differentiating among these three avocado ecotypes.

2. Materials and Methods

2.1. Plant Materials

The three avocado ecotypes included in this study were obtained from the Chinese Academy of Tropical Agricultural Sciences: Mexican (Walter Hole), Guatemalan (Nabal), and West Indian (Donnie). For each ecotype, the fruits were collected from six 10-year-old healthy individuals with Zutano clonal rootstock in September 2020 (two trees were classified as a unit for each biological replicate). After reaching physiological maturity (i.e., able to ripen after harvest), two sets of 10 avocado fruits were randomly collected for each biological replicate. The first set was lyophilized for an oil body analysis, whereas the second set was analyzed for the fatty acid compositions, lipid and other metabolites, and gene expression.

2.2. Analysis of the Fatty Acid Composition by Gas Chromatography–Mass Spectrometry

The mesocarps of ten avocado fruits were combined to form one biological replicate and homogenized using a high-speed homogenizer for the subsequent extraction of fatty acids. The fatty acid compositions were determined using the GC-MS method described by Ge et al. [20]. Similarly, qualitative and quantitative analyses of fatty acid compositions were performed according to the method described by Ge et al. [20]. The FAME contents (expressed as mg/g dry weight) for each ecotype were calculated as the mean \pm standard deviation of three biological replicates, each comprising two technical replicates.

2.3. Histological Analyses

To visualize lipid droplets in the mature avocado mesocarps of the three ecotypes, samples 10–15 mm thick were prepared using the CV5030 vibratome and washed three times with 0.2 M phosphate-buffered saline. They were then stained with 0.5 mg/mL Nile red and examined using the Zeiss LM510 confocal microscope, with a laser excitation at 543 nm and a 10 \times objective lens.

2.4. RNA Extraction and Quantitative Real-Time PCR (qRT-PCR)

For each ecotype, total RNA was extracted from the mature avocado mesocarp, as described by Ge et al. [20]. In total, 12 highly transcribed lipid-related genes participating in FA synthesis and TAG storage, with average transcript levels exceeding 100 FPKM/stage during five avocado mesocarp developmental stages, were selected based on the results of one of our previous study [20]. The expression of these 12 lipid-related genes involved in FA synthesis and TAG storage was analyzed by qRT-PCR, with *PaActin7* used as the internal control. The sequences of these genes were obtained from the reference genome [21]. The cDNA concentration was determined, after which the cDNA was diluted to 12.5 ng/ μ L. The qRT-PCR assay was completed as described by Ge et al. [20]. Relative gene expression levels were determined using the $2^{-\Delta\Delta C_t}$ method [22]. Data are presented herein as the mean \pm standard deviation of three biological replicates, each comprising two technical replicates. The qRT-PCR primers are listed in Supplementary Table S1.

2.5. Analysis of the Lipids by Ultra-High-Performance Liquid Chromatography-Triple and Time-of-Flight Mass Spectrometry

The mesocarps of 10 avocado fruits were combined (one biological replicate) and homogenized using a high-speed homogenizer, after which the lipids were extracted. The 20 mg of sample was weighted to an EP tube after freeze-drying, and 1000 μ L extract solution (acetonitrile:methanol:water = 2: 2:1) containing 1 μ g/mL internal standard was added. After 30 s vortex, the samples were homogenized at 35 Hz for 4 min and sonicated for 5 min in an ice-water bath. The homogenization and sonication cycle was repeated 3 times. Then the samples were incubated for 1 h at -40 $^{\circ}$ C and centrifuged at 12,000 rpm for 15 min at 4 $^{\circ}$ C. The resulting supernatant was transferred to a fresh glass.

LC-MS/MS analyses were performed using an UHPLC system (1290, Agilent Technologies) with a UPLC HSS T3 column (2.1 mm \times 100 mm, 1.8 μ m) coupled to Q Exactive mass spectrometer (Thermo). The mobile phase A was 0.1% formic acid in water for positive mode, and 5 mmol/L ammonium acetate in water for negative mode, and the mobile phase B was acetonitrile. The elution gradient was set as follows: 0~1.0 min, 1% B; 1.0~8.0 min, 1%~99% B; 8.0~10.0 min, 99% B; 10.0~10.1 min, 99%~1% B; 10.1~12 min, 1% B. The flow rate was 0.5 mL/min. The injected volume was 2 μ L. The QE mass spectrometer was used for its ability to acquire MS/MS spectra on information-dependent acquisition (IDA) mode in the control of the acquisition software (Xcalibur 4.0.27, Thermo). In this mode, the acquisition software continuously evaluates the full scan MS spectrum. The ESI source conditions were set as following: sheath gas flow rate as 45 Arb, Aux gas flow rate as 15 Arb, capillary temperature 400 $^{\circ}$ C, full MS resolution as 70,000, MS/MS resolution as 17,500, collision energy as 20/40/60 in NCE mode, spray Voltage as 4.0 kV (positive) or -3.6 kV (negative), respectively.

The raw data were converted to the mzXML format using ProteoWizard and processed with an in-house program, which was developed using R and based on XCMS, for peak detection, extraction, alignment, and integration. Then, an in-house MS2 database (BiotreeDB) was applied in metabolite annotation. The cutoff for annotation was set at 0.3. The relative contents of lipid metabolite were calculated as the mean \pm standard deviation of three biological replicates.

Differential metabolites were searched in the pathway database of the Kyoto encyclopedia of genes and genomes (KEGG). KEGG annotation analysis can only find the pathways involved in all differential metabolites, and then map KEGG, PubChem, and other authoritative metabolites databases through differential metabolites.

2.6. Analysis of the Metabolites by Ultra-High Performance Liquid Chromatography-Q Exactive-Mass Spectrometry

The mesocarps of 10 avocado fruits were combined (one biological replicate) and homogenized using a high-speed homogenizer, after which the metabolites were extracted. The 25 mg of sample was weighted to an EP tube. 200 μ L water, 480 μ L extract solution

(MTBE:MeOH = 5:1) were added sequentially. The samples were homogenized at 35 Hz for 4 min and sonicated for 5 min in ice-water bath. The homogenization and sonication cycle was repeated 3 times. Then the samples were incubated at $-40\text{ }^{\circ}\text{C}$ for 1 h and centrifuged at 3000 rpm for 25 min at $4\text{ }^{\circ}\text{C}$. 350 μL of supernatant was transferred to a fresh tube and dried in a vacuum concentrator at $37\text{ }^{\circ}\text{C}$. Then, the dried samples were reconstituted in 200 μL of 50% methanol in dichloromethane by sonication for 10 min in ice-water bath. The constitution was then centrifuged at 13,000 rpm for 15 min at $4\text{ }^{\circ}\text{C}$, and 75 μL of supernatant was transferred to a fresh glass vial for LC/MS analysis.

The UHPLC separation was carried out using a ExionLC Infinity series UHPLC System (AB Sciex), equipped with a Kinetex C18 column ($2.1 \times 100\text{ mm}$, $1.7\text{ }\mu\text{m}$, Phenomen). The mobile phase A consisted of 40% water, 60% acetonitrile, and 10 mmol/L ammonium formate. The mobile phase B consisted of 10% acetonitrile and 90% isopropanol, which was added with 50 mL 10 mmol/L ammonium formate for every 1000 mL mixed solvent. The analysis was carried with elution gradient as follows: 0~12.0 min, 40%~100% B; 12.0~13.5 min, 100% B; 13.5~13.7 min, 100%~40% B; 13.7~18.0 min, 40% B. The column temperature was $55\text{ }^{\circ}\text{C}$. The auto-sampler temperature was $6\text{ }^{\circ}\text{C}$, and the injection volume was 2 μL (pos) or 2 μL (neg), respectively.

The TripleTOF 5600 mass spectrometer was used for its ability to acquire MS/MS spectra on an information-dependent basis (IDA) during an LC/MS experiment. In this mode, the acquisition software (Analyst TF 1.7, AB Sciex) continuously evaluates the full scan survey MS data, as it collects and triggers the acquisition of MS/MS spectra depending on preselected criteria. In each cycle, the most intensive 12 precursor ions with intensity above 100 were chosen for MS/MS at collision energy (CE) of 45 eV (12 MS/MS events with accumulation time of 50 msec each). ESI source conditions were set as following: Gas 1 as 60 psi, Gas 2 as 60 psi, Curtain Gas as 30 psi, Source Temperature as $600\text{ }^{\circ}\text{C}$, de-clustering potential as 100 V, Ion Spray Voltage Floating (ISVF) as 5000 V or -3800 V in positive or negative modes, respectively.

The raw data files (.wiff format) were converted to files in mzXML format using the 'msconvert' program from ProteoWizard. Peak detection was first applied to the MS1 data. The CentWave algorithm in XCMS was used for peak detection, With the MS/MS spectrum, lipid identification was achieved through a spectral match using LipidBlast library. The relative contents of metabolites were calculated as the mean \pm standard deviation of three biological replicates.

3. Results

3.1. Comparative Analysis of the Oil Content in the Mature Avocado Mesocarps of Three Ecotypes

The differences in the lipid droplet abundance in the mature mesocarps of three avocado ecotypes were analyzed at the cellular level by confocal microscopy (Figure 1). The mature mesocarp sections were stained with Nile red, which selectively stains lipid droplets, enabling the evaluation of the differences in the lipid droplet compartmentalization among the mature mesocarp tissues of the three ecotypes. The fluorescence area was greatest for the Mexican ecotype (Walter Hole), followed by the Guatemalan ecotype (Nabal) and then the West Indian ecotype (Donnie). Thus, the rank order for the compartmentalization of lipid droplets per unit tissue area was as follows: Mexican ecotype (Walter Hole) > Guatemalan ecotype (Nabal) > West Indian ecotype (Donnie) (Figure 1).

The fatty acid compositions of the mature avocado mesocarps of three ecotypes were determined by GC-MS. The same six fatty acids were founded in the mature mesocarps of all three ecotypes, and palmitic, stearic, oleic, and linolenic acids differed significantly among the ecotypes, respectively (Duncan, $p \leq 0.05$) (Figure 2a). In this study, the total oil content was calculated as the total content of all six fatty acid components. A comparison of the total oil contents revealed significant differences among the three ecotypes (Duncan, $p \leq 0.05$), with the highest oil content detected for the Mexican ecotype (Walter Hole), followed by the Guatemalan ecotype (Nabal) and then the West Indian ecotype (Donnie) (Figure 2b). The differences in the total oil contents among the mature avocado mesocarps

of the three ecotypes were consistent with the differences in the lipid droplet areas. Additionally, in all mature avocado mesocarps, most major fatty acids were significantly more abundant in the Mexican ecotype (Walter Hole) than in the other two ecotypes, with the lowest levels detected for the West Indian ecotype (Donnie) (Figure 2a).

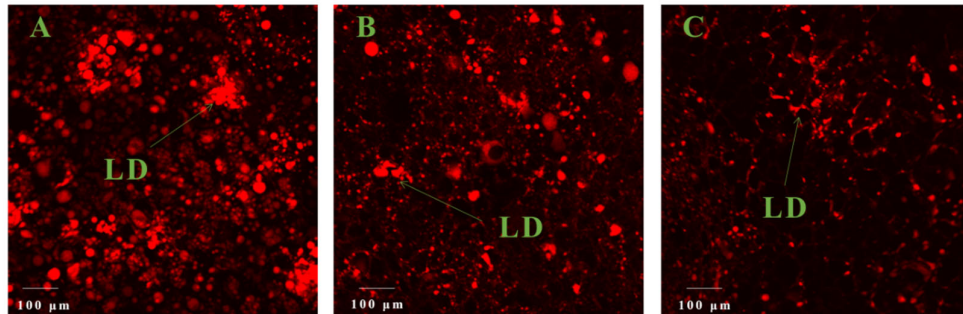


Figure 1. Confocal microscopy images of lipid droplets in the mature mesocarps of three avocado ecotypes. (A) Mexican ecotype (Walter Hole); (B) Guatemalan ecotype (Nabal); (C) West Indian ecotype (Donnie). Lipid droplets were visualized by Nile red staining. LD: lipid droplet.

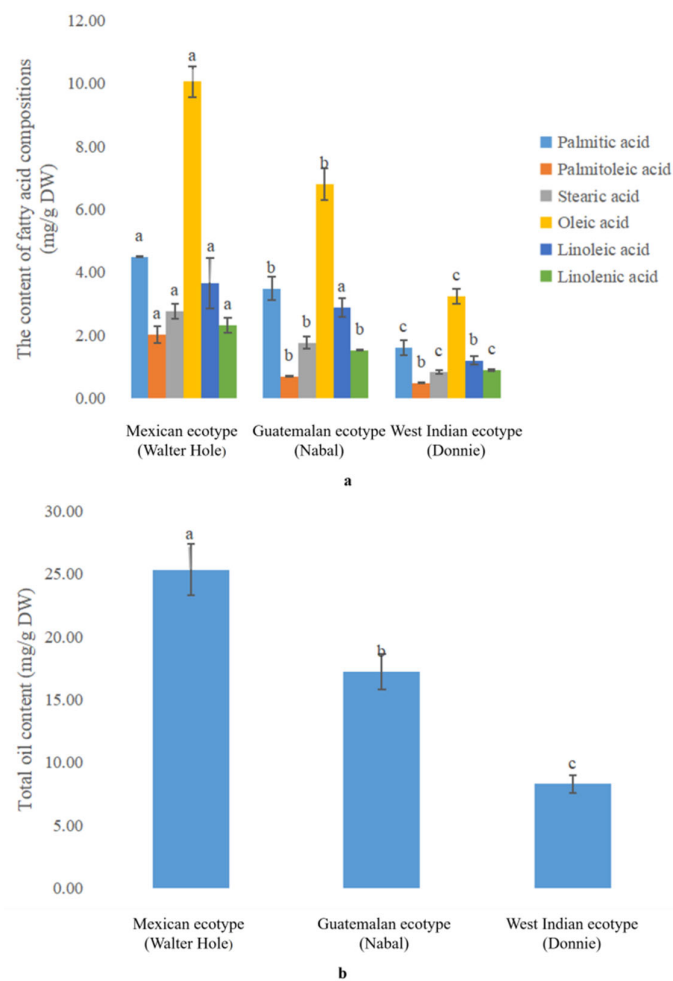


Figure 2. Total oil contents and fatty acid compositions of the mature avocado mesocarps of three ecotypes. (a) Fatty acid compositions in the mature avocado mesocarps; (b) Total oil contents in the mature avocado mesocarps. Error bars indicate standard deviation from three biological replicates with two technical replicates of each. Means with different letters in the same color histogram indicate significant differences (Duncan, $p \leq 0.05$).

3.2. Expression-Level Changes to Lipid-Related Genes Involved in FA Synthesis and TAG Storage among the Mature Avocado Mesocarps of Three Ecotypes

The expression levels of nine genes involving in FA synthesis and three associated with TAG storage in the mature avocado mesocarps were determined via qRT-PCR, which revealed significant differences in the expression of most of the lipid-related genes among the three ecotypes (Duncan, $p \leq 0.05$) (Figure 3).

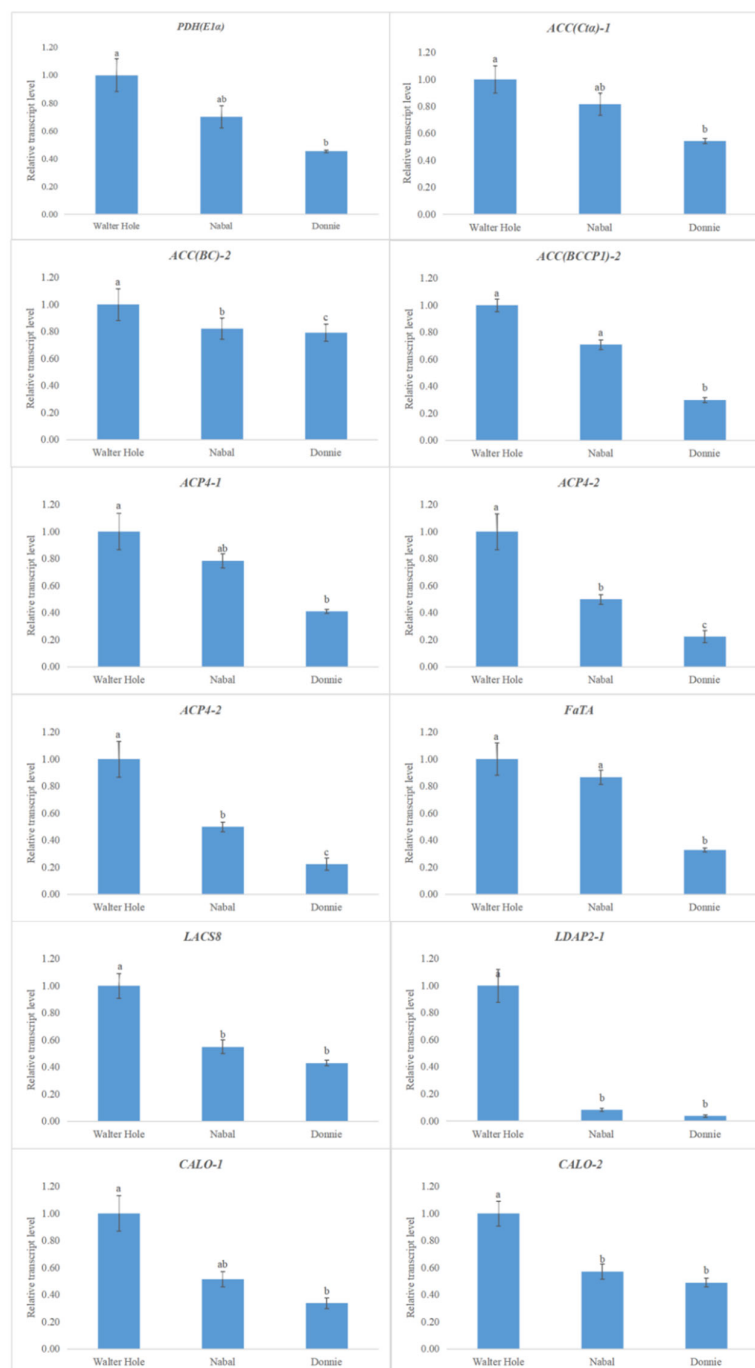


Figure 3. Relative expression patterns of twelve lipid-related genes involved in FA synthesis and TAG storage in the mature avocado mesocarps of three ecotypes. Error bars indicate standard deviation from three biological replicates with two technical replicates of each. Means with different letters in the same color histogram indicate significant differences (Duncan, $p \leq 0.05$).

For a more thorough analysis, the fatty acid profiles and the expression levels of nine lipid-related genes involving in FA synthesis in the mature avocado mesocarps of three ecotypes underwent a correlation analysis. The transcript levels of the nine lipid-related genes were all positively correlated with the six fatty acid profiles, suggesting these genes affect fatty acid accumulation (Supplementary Table S2). Notably, the *ACC (Cta)-1*, *ACC (BCCP1)-2*, and *ACP4-1* transcript levels were highly correlated with the palmitic acid content, whereas the *ACC (BC)-2*, *SAD (FAB2)*, and *LACS8* expression levels were markedly correlated with the abundance of palmitoleic acid. However, only the *PDH (E1 α)* transcript level was significantly correlated with the stearic acid content. Moreover, the transcript levels of two genes, *PDH (E1 α)* and *ACC (BCCP1)-2*, were correlated with the oleic acid level, whereas the expression levels of *ACP4-1* and *PDH (E1 α)* were correlated with the linoleic and linolenic acid contents, respectively. Besides, in the present study, the expression-level changes to three lipid-related genes associated with TAG storage were also consistent with the lipid droplet areas in the mature avocado mesocarps of the three ecotypes.

3.3. Lipids Differences among the Mature Avocado Mesocarps of Three Ecotypes

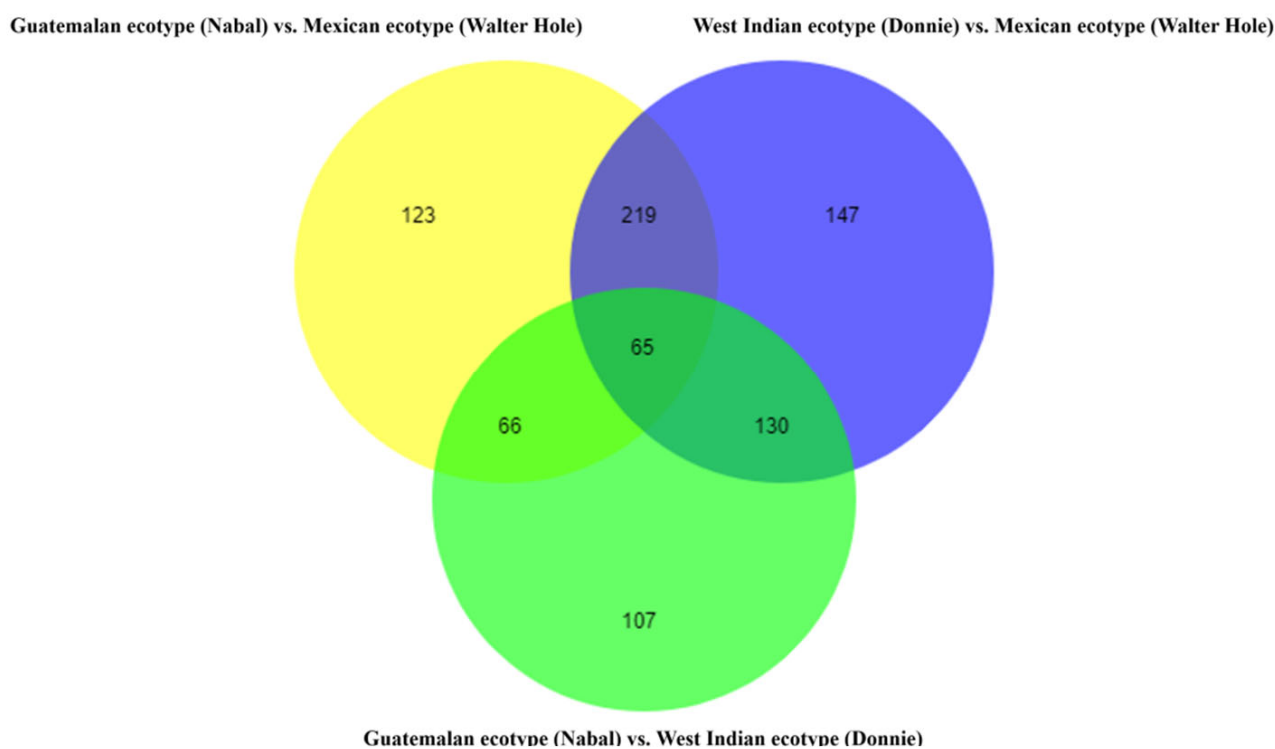
A UHPLC-Q-TOF-MS system was used to evaluate the lipid compositions in the mature avocado mesocarps of three ecotypes. A comparison of the mass spectra of the analytes with those of commercial reference standard compounds resulted in the identification of 1099 lipid components in the three avocado ecotypes, including 147 diacylglycerols (DAG), 1078 TAGs, 90 galactolipids (GL), and 384 phospholipids (PL) (Table S3). As shown in Table S3, monogalactosyldiacylglycerol (MGDG) and digalactosyldiacylglycerol (DGDG) were two dominant GLs in the three avocado ecotypes, and phosphatidic acid (PA), phosphatidylcholine (PC), phosphatidylethanolamine (PE), phosphatidylglycerol (PG), phosphatidylinositol (PI), and phosphatidylserine (PS) were six major PLs in the three avocado ecotypes. The data were subjected to a PCA, which clearly separated the three avocado ecotypes in the PC1 \times PC2 score plots (Figure S1). The first two PCs accounted for 44.90% of the total variance in the data. On the basis of these results, we used the first two components to examine the avocado lipid profiles.

During pairwise comparisons, significant differences between lipids were determined based on the following criteria: a variable importance in projection value > 1 , p -value < 0.01 , and a fold-change > 2 or < 0.5 . Significant differences among the three avocado ecotypes were detected for 857 lipids from the following 10 lipid classes: DAGs, TAGs, MGDGs, DGDGs, PAs, PCs, PEs, PGs, PIs, and PSs (Table S4). The relative contents of most of 10 lipid classes differed significantly among the three avocado ecotypes (Duncan, $p \leq 0.05$) (Table 1). The relative content of four classes (DAG, TAG, PC, and PI) presented much higher levels in the Mexican ecotype (Walter Hole) than those in other two ecotypes, and only one class (DGDG) was higher in the West Indian ecotype (Donnie) compared to other two ecotypes. The remaining five classes (MGDG, PA, PE, PG, and PS) displayed the highest relative contents in the Guatemalan ecotype (Nabal). Among the 857 differentially accumulated lipids, the relative contents of 65 lipids differed in all analyzed avocado ecotypes, including six DAGs, 40 TAGs, two MGDGs, four DGDGs, four PCs, seven PEs, and two PGs (Figure 4). These 65 lipids were showed in red in Table S3. The profiles of these lipids might be potential candidate biomarkers useful for identifying diverse avocado ecotypes.

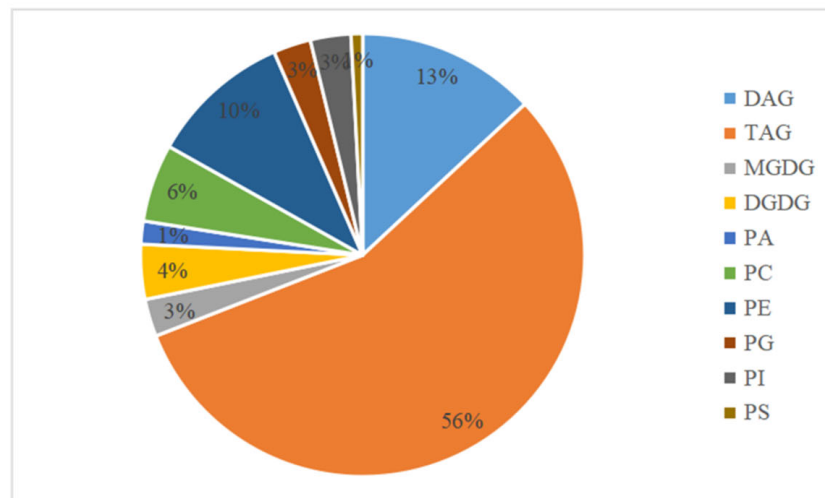
Table 1. Relative contents of ten classes comprising 857 lipids detected in the mature avocado mesocarps of three ecotypes.

Lipid Classes	Relative Total Amount		
	Mexican Ecotype (Walter Hole)	Guatemalan Ecotype (Nabal)	West Indian Ecotype (Donnie)
DAG	$2.98 \times 10^{-2} \pm 1.41 \times 10^{-4}$ a	$1.93 \times 10^{-0.2} \pm 4.06 \times 10^{-4}$ b	$1.55 \times 10^{-0.2} \pm 6.27 \times 10^{-4}$ b
TAG	$2.47 \times 10^{-2} \pm 2.65 \times 10^{-4}$ a	$2.13 \times 10^{-2} \pm 2.67 \times 10^{-4}$ b	$2.03 \times 10^{-2} \pm 8.61 \times 10^{-4}$ b
MGDG	$6.74 \times 10^{-2} \pm 5.58 \times 10^{-4}$ a	$9.03 \times 10^{-3} \pm 9.23 \times 10^{-4}$ b	$5.51 \times 10^{-3} \pm 4.06 \times 10^{-4}$ a
DGDG	$3.83 \times 10^{-3} \pm 2.15 \times 10^{-4}$ a	$6.20 \times 10^{-3} \pm 1.92 \times 10^{-4}$ b	$6.60 \times 10^{-3} \pm 2.94 \times 10^{-4}$ b
PA	$3.54 \times 10^{-4} \pm 3.07 \times 10^{-5}$ a	$8.42 \times 10^{-4} \pm 3.68 \times 10^{-5}$ b	$6.37 \times 10^{-4} \pm 7.34 \times 10^{-5}$ c
PC	$5.24 \times 10^{-3} \pm 1.05 \times 10^{-3}$ a	$3.77 \times 10^{-2} \pm 5.12 \times 10^{-3}$ b	$2.71 \times 10^{-2} \pm 3.87 \times 10^{-3}$ b
PE	$1.47 \times 10^{-2} \pm 1.49 \times 10^{-3}$ a	$3.64 \times 10^{-2} \pm 1.90 \times 10^{-3}$ b	$3.12 \times 10^{-2} \pm 1.90 \times 10^{-4}$ b
PG	$2.51 \times 10^{-3} \pm 3.97 \times 10^{-4}$ a	$2.75 \times 10^{-3} \pm 1.35 \times 10^{-4}$ a	$2.13 \times 10^{-3} \pm 1.33 \times 10^{-4}$ a
PI	$8.09 \times 10^{-4} \pm 3.95 \times 10^{-5}$ a	$6.15 \times 10^{-4} \pm 3.45 \times 10^{-5}$ b	$4.59 \times 10^{-4} \pm 2.33 \times 10^{-5}$ c
PS	$1.68 \times 10^{-4} \pm 1.00 \times 10^{-5}$ a	$3.59 \times 10^{-4} \pm 4.18 \times 10^{-5}$ b	$2.82 \times 10^{-4} \pm 2.65 \times 10^{-5}$ c

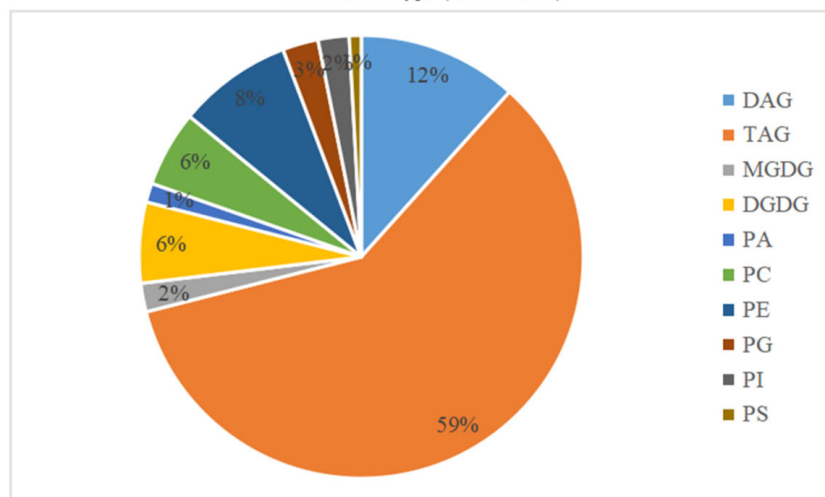
Error bars indicate standard deviation from three biological replicates of each ecotype. Means with the different letters indicate significant differences (Duncan, $p \leq 0.05$) among mature avocado mesocarp of three ecotypes.

**Figure 4.** Detection of 857 differentially accumulated lipids in the mature avocado mesocarps of three ecotypes.

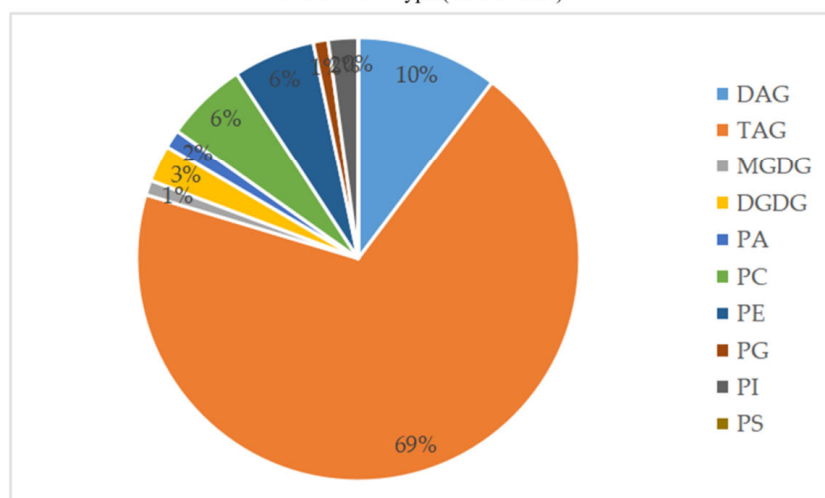
Significant differences in the relative contents of 473, 561, and 368 lipids were revealed in the Guatemalan ecotype (Nabal) vs. Mexican ecotype (Walter Hole), the West Indian ecotype (Donnie) vs. Mexican ecotype (Walter Hole), and the Guatemalan ecotype (Nabal) vs. West Indian ecotype (Donnie) comparisons, respectively (Table S4). In these pairwise comparisons, the dominating class with differentially accumulated lipids was always TAGs (Figure 5). The lipids with relative contents that differed by a factor of 10,000 between ecotypes were identified as TAG 16:0-17:1-18:1 and TAG 17:1-18:1-19:2 (TAG) (Guatemalan ecotype (Nabal) vs. Mexican ecotype (Walter Hole)), as well as (West Indian ecotype (Donnie) vs. Mexican ecotype (Walter Hole)). The fold-changes in the relative contents of differentially accumulated lipids were substantially lower for the Guatemalan ecotype (Nabal) vs. West Indian ecotype (Donnie) comparison than for the other pairwise comparisons, with the minimal fold-change (7753) detected for TAG 14:1-14:1-18:5 (TAG) (Table S4).



(a) The numbers of ten differentially lipid classes between Guatemalan ecotype (Nabal) and Mexican ecotype (Walter Hole)



(b) The numbers of ten differentially lipid classes between West Indian ecotype (Donnie) and Mexican ecotype (Walter Hole)



(c) The numbers of ten differentially lipid classes between Guatemalan ecotype (Nabal) and West Indian ecotype (Donnie)

Figure 5. Proportion of differentially accumulated lipids in ten classes among the mature avocado mesocarps of three ecotypes.

3.4. Metabolites Differences among the Mature Avocado Mesocarps of Three Ecotypes

A UHPLC-QE-MS system was used to evaluate the other metabolite compositions in the mature avocado mesocarps of three ecotypes. A comparison of the mass spectra of the analytes with those of commercial reference standard compounds resulted in the identification of 522 other metabolites in the three avocado ecotypes (Table S5). The data were subjected to a PCA, which clearly separated the three avocado ecotypes in the PC1 × PC2 score plots (Figure S2). The first two PCs accounted for 68.20% of the total variance in the data. On the basis of these results, we used the first two components to examine the avocado metabolite profiles.

During pairwise comparisons, significant differences between other metabolites were determined based on the following criteria: a variable importance in projection value > 1, *p*-value < 0.01, and a fold-change >2 or <0.5. Significant differences among the three avocado ecotypes were detected for 248 other metabolites from the following seven metabolite super-classes: benzenoids, hydrocarbons, lipids and lipid-like molecules, organic acids and derivatives, organic oxygen compounds, organic heterocyclic compounds, and phenylpropanoids and polyketides (Table S6). The relative contents of most of seven metabolite super-classes differed significantly among the three avocado ecotypes (Duncan, *p* ≤ 0.05) (Table 2). The relative content of only one superclass (lipids or lipid-like molecules) was higher in the Mexican ecotype (Walter Hole) compared to other two ecotypes, and two super-classes (benzenoids and phenylpropanoids and polyketides) presented much higher levels in the Guatemalan ecotype (Nabal) than those in other two ecotypes. The remaining four super-classes (hydrocarbons, organic acids and derivatives, organic oxygen compounds, and organic heterocyclic compounds) displayed the highest relative contents in the West Indian ecotype (Donnie). Among the 248 differentially accumulated other metabolites, the relative contents of 15 other metabolites differed in all analyzed avocado ecotypes, including two benzenoids (2,6-di-tert-butyl-4-methylphenol and (12)-gingerdione), six lipids or lipid-like molecules (MG(0:0/18:3(6Z,9Z,12Z)/0:0, dexamethasone, isopulegol acetate, PSF-A, physalin E, and stearidonyl carnitine), two organic acids or derivatives (3-nitrotyrosine and N-acetyl-L-phenylalanine), five organic oxygen compounds (chlorogenic acid, galactaric acid, syoyualdehyde, colupulone, and phenylethyl primeveroside) (Figure 6). The profiles of these metabolites might be potential candidate biomarkers useful for identifying diverse avocado ecotypes.

Table 2. Relative contents of seven super-classes comprising 248 metabolites detected in the mature avocado mesocarps of three ecotypes.

Metabolite Super-Classes	Relative Total Amount		
	Mexican Ecotype (Walter Hole)	Guatemalan Ecotype (Nabal)	West Indian Ecotype (Donnie)
Benzenoids	15.06 ± 0.51 a	22.01 ± 1.35 b	19.52 ± 1.93 b
Hydrocarbons	0.79 ± 0.06 a	3.15 ± 0.13 b	3.55 ± 0.29 b
Lipids and lipid-like molecules	135.18 ± 3.75 a	93.86 ± 4.88 b	84.99 ± 5.53 b
Organic acids and derivatives	40.14 ± 4.43 a	26.82 ± 2.05 b	45.99 ± 2.30 a
Organic oxygen compounds	199.28 ± 10.39 a	523.53 ± 37.08 b	567.93 ± 34.98 b
Organic heterocyclic compounds	22.57 ± 2.58 a	22.64 ± 1.67 a	23.63 ± 0.63 a
Phenylpropanoids and polyketides	0.78 ± 0.08 a	5.07 ± 0.67 b	1.06 ± 0.23 a

Error bars indicate standard deviation from three biological replicates of each ecotype. Means with the different letters indicate significant differences (Duncan, *p* ≤ 0.05) among mature avocado mesocarp of three ecotypes.

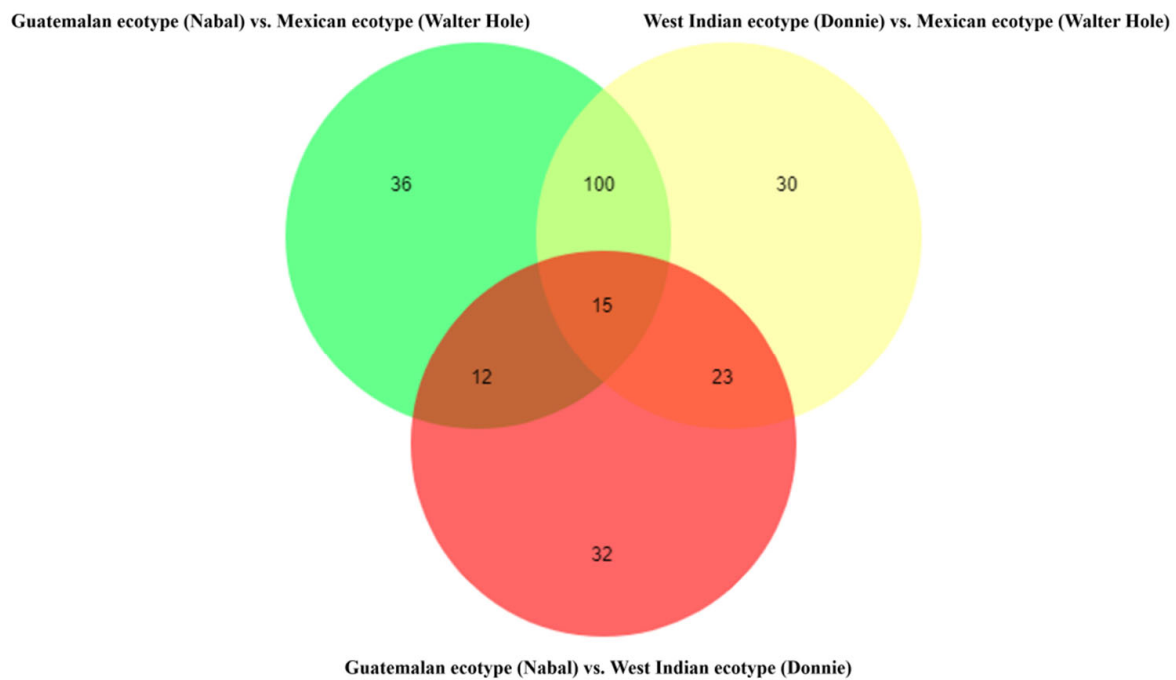
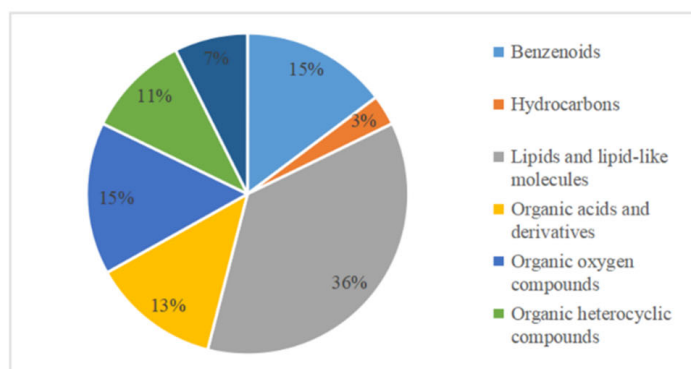
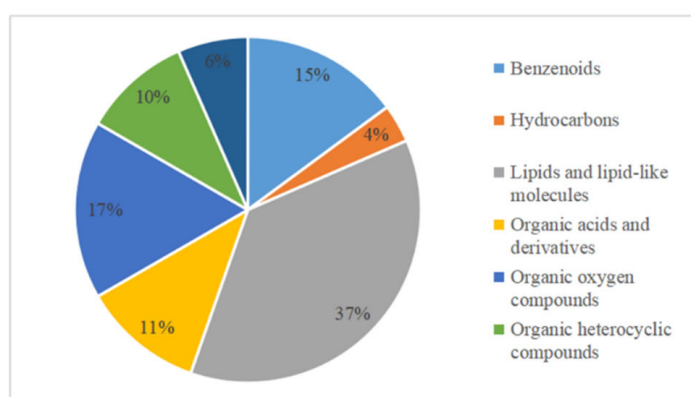


Figure 6. Detection of 248 differentially accumulated metabolites in the mature avocado mesocarps of three ecotypes.

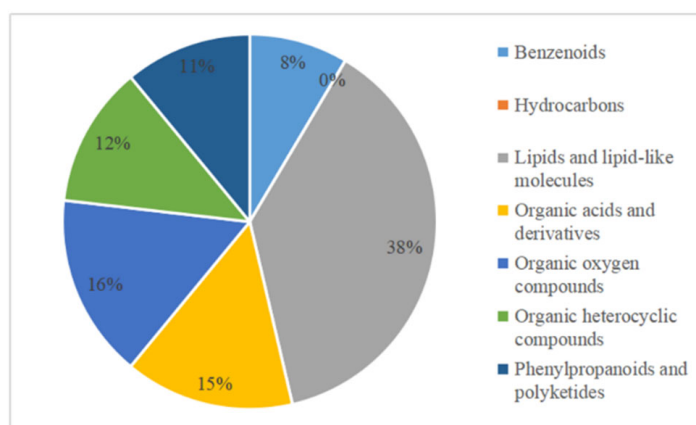
Significant differences in the relative contents of 163, 168, and 82 other metabolites were revealed in the Guatemalan ecotype (Nabal) vs. Mexican ecotype (Walter Hole), the West Indian ecotype (Donnie) vs. Mexican ecotype (Walter Hole), and the Guatemalan ecotype (Nabal) vs. West Indian ecotype (Donnie) comparisons, respectively (Table S6). In these pairwise comparisons, the main super-class with differentially accumulated metabolites was always lipids and lipid-like molecules (Figure 7). The metabolites with relative contents that differed by a factor of 10,000 between ecotypes were identified as adrenic acid (lipid or lipid-like molecule), ethyl isopropyl ketone (organic oxygen compound), and 2'-O-methylcajanone (phenylpropanoid or polyketide) (Guatemalan ecotype (Nabal) vs. Mexican ecotype (Walter Hole)), as well as geranyl-PP and jasmonic acid (lipid or lipid-like molecules) and ethyl isopropyl ketone (organic oxygen compound) (West Indian ecotype (Donnie) vs. Mexican ecotype (Walter Hole)). The fold-changes in the relative contents of differentially accumulated metabolites were substantially lower for the Guatemalan ecotype (Nabal) vs. West Indian ecotype (Donnie) comparison than for the other pairwise comparisons, with the maximal fold-change (92) detected for scopoletin (phenylpropanoid or polyketide) (Table S6).



(a) The numbers of seven differentially metabolite superclasses between Guatemalan ecotype (Nabal) and Mexican ecotype (Walter Hole)



(b) The numbers of seven differentially metabolite superclasses between West Indian ecotype (Donnic) and Mexican ecotype (Walter Hole)



(c) The numbers of seven differentially metabolite superclasses between Guatemalan ecotype (Nabal) and West Indian ecotype (Donnic)

Figure 7. Proportion of differentially accumulated metabolites in seven super-classes among the mature avocado mesocarps of three ecotypes.

3.5. Metabolic Pathway Analysis of Differentially Accumulated Metabolites

The KEGG metabolic pathway database is a useful resource for investigating metabolites and metabolic networks because it provides information regarding diverse cellular synthesis and degradation processes in diagrammatic forms. In the current study, a comprehensive analysis uncovered differences in the changes to the metabolic pathways among the mature avocado mesocarps of the three examined ecotypes (Figure 8). More specifically, significant differences were detected in the tyrosine metabolism between the Guatemalan ecotype (Nabal) and the Mexican ecotype (Walter Hole), in the glyoxylate and dicarboxy-

late metabolism, tyrosine metabolism, and isoquinoline alkaloid biosynthesis between the West Indian ecotype (Donnie) and the Mexican ecotype (Walter Hole), and in the phenylalanine metabolism between the Guatemalan ecotype (Nabal) and the West Indian ecotype (Donnie).

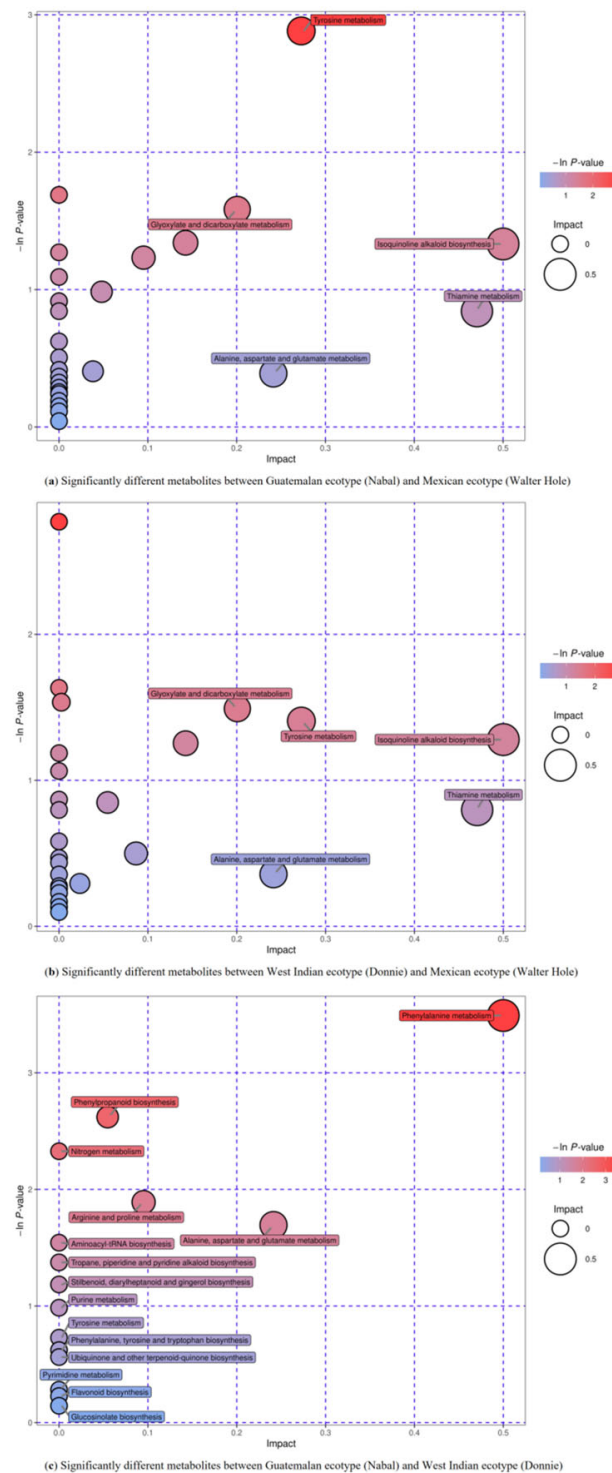


Figure 8. Overview of the analysis of metabolic pathways among the mature avocado mesocarps of three ecotypes. The y -axis ($-\ln(p\text{-value})$) indicates the significance of the metabolic pathway enrichment. The x -axis indicates the impact of the pathway as determined by the Pathway Topology Analysis.

4. Discussion

The oil content is widely perceived as distinguishing character among three avocado ecotypes [3]. In the present study, the oil content character were systematically analyzed in the three avocado ecotypes from multi-dimensional support for the first time, and the variation in the oil content was confirmed among the examined ecotypes. Similarly, in the current study, the UHPLC-Q-TOF-MS and UHPLC-QE-MS analyses identified 1099 lipids and 522 other metabolites in avocado mesocarps. The lipid and other metabolites of the three avocado ecotypes were clearly separated in the PCA, reflecting the diversity in the metabolites among the examined ecotypes.

Lipid droplets accumulating TAG are encircled by a phospholipid monolayer and abundant amphipathic proteins, and they function as the hub for metabolic processes [23]. An earlier study proved that *OBO*, *STERO*, and *CALO* are TAG storage-related genes [24]. Recently, new lipid droplet-associated genes have been identified, namely *LDAP1* and *LDAP2* [25,26]. In an earlier study, we proved that *PaLDAP2-1* and two *PaCALO* paralogs are TAG storage-related genes [20]. In the present study, the expression-level changes to three lipid-related genes associated with TAG storage were consistent with the lipid droplet areas in the mature avocado mesocarps of the three ecotypes.

The Mexican ecotype is generally considered to produce a lower-quality fruit than the other two analyzed ecotypes. Accordingly, it is usually used as rootstock [27]. Our metabolomic analysis revealed that compared with the other ecotypes with moderate or low oil contents, the Mexican ecotype (Walter Hole), which has a relatively high oil content, has a greater abundance of lipids and lipid-like molecules, but a lower abundance of organic heterocyclic compounds, benzenoids, hydrocarbons, organic oxygen compounds, and phenylpropanoids and polyketides. Therefore, the low fruit quality of the Mexican ecotype may be at least partly due to the lower metabolite contents in the avocado mesocarp. The fruit of the Guatemalan ecotype, which is popular among consumers in temperate and subtropical regions, has good pulp quality and flavor, as well as a soft texture [28,29]. Regarding the Guatemalan ecotype (Nabal) included in this study, its oil and metabolite contents were generally between the corresponding contents of the Mexican (Walter Hole) and West Indian (Donnie) ecotypes. It also had a distinct metabolite profile. The relative benzenoid, phenylpropanoid, and polyketide contents were highest in the Guatemalan ecotype (Nabal), whereas the abundance of the organic acids and derivatives had the opposite trend. The relative balance between the oil content and the abundance of most other metabolites may influence the substantial nutritional value and good organoleptic properties of the Guatemalan ecotype mesocarp. The fruit of the West Indian ecotype, which is mainly consumed by people in tropical regions, has a fair-to-good pulp quality and a low oil content [3]. The West Indian ecotype (Donnie) examined in this study was relatively abundant with hydrocarbons, organic oxygen compounds, organic heterocyclic compounds, and organic acids and derivatives, which may contribute to the good-to-excellent quality of its pulp, which has a unique flavor. Additionally, because of its low calorie content, the West Indian fruit is currently marketed as a heart-healthy alternative to the fruits with high oil contents produced by other avocado cultivars.

Lipidome data obtained by UHPLC-Q-TOF-MS analysis illustrate a detailed profiling of DAGs, TAGs, GLs, and PLs present in avocado mesocarp derived from three ecotypes. In the present study, the quantities and relative contents of DAGs and TAGs were all higher than those of GLs and PLs. Similar lipid profiles were detected in DAGs and TAGs among three avocado ecotypes. This could reveal that DAGs might be the precursors for TAGs from PC-derived DAG versus de novo DAG via the Kennedy pathway, which was also confirmed by Zhi et al. [19] and Lu et al. [30]. Relative to other two ecotypes, much higher levels of DAGs and TAGs were detected in the Mexican (Walter Hole), suggesting a highly active DAGs and TAGs recycling therein. Besides, considering the similar profiles among DGDGs, PAs, PEs, and PSs in avocado mesocarp, it was tempting to suggest that avocado mesocarp may facilitate the inter-conversion of among DGDGs, PAs, PEs, and PSs. Unlike DAGs and TAGs, two GLs classes (MGDG and DGDG) and four dominating PLs classes

(PAs, PEs, PGs, and PSs) displayed the highest levels in the Guatemalan ecotype (Nabal) compared to other two ecotypes. So, perhaps in this study, it suggested that there was differences between DAG and TAG biosyntheses and GL and PL biosyntheses.

5. Conclusions

In this study, comprehensive biochemical, histological, and gene expression analyses elucidated the differences in the oil content among three avocado ecotypes. Furthermore, the lipid and metabolite profiles of the three avocado ecotypes were measured through UHPLC-Q-TOF-MS and UHPLC-QE-MS, and the 1099 lipids and 522 other metabolites were detected and classified into specific groups, respectively. The results of pairwise comparisons indicated the 65 lipids and 15 other metabolites varied among the three avocado ecotypes. The data generated in this study may be relevant for clarifying the differences in fatty acids, lipids, and other metabolites among the three avocado ecotypes.

Supplementary Materials: The following are available online at <https://www.mdpi.com/article/10.3390/horticulturae7050094/s1>, Table S1: Primers used in qRT-PCR; Table S2: Correlation coefficients for expressions of nine lipid-related genes participating in FA synthesis and fatty acid levels in mature avocado mesocarp of three ecotypes; Table S3: Lipidomic data measured in three avocado ecotypes; Table S4: Differentially accumulated lipids in pairwise comparison among three avocado ecotypes; Table S5: Metabolite data measured in three avocado ecotypes; Table S6: Differentially accumulated metabolites in pairwise comparison among three avocado ecotypes; Figure S1: PCA scores plot for Mexican ecotype (Walter Hole) (red circle), Guatemalan ecotype (Nabal) (purple diamond), and West Indian ecotype (Donnie) (blue square); Figure S2: PCA scores plot for Mexican ecotype (Walter Hole) (red circle), Guatemalan ecotype (Nabal) (purple diamond), and West Indian ecotype (Donnie).

Author Contributions: Conceptualization, Y.G.; validation, X.Z. and Y.L. (Yuanzheng Liu); formal analysis, X.Z., Y.L. (Yuanzheng Liu), and L.W.; resources, J.W. and Y.L. (Yanxia Li); writing—original draft preparation, Y.G.; project administration, Y.G.; funding acquisition, Y.G. and W.M. All authors have read and agreed to the published version of the manuscript.

Funding: This research was funded by the Natural Science Foundation of Hainan Province of China (grant number 2019RC264) and Budget Items of Ministry of Agriculture and Rural Affairs (grant number 20213578).

Institutional Review Board Statement: Not applicable.

Informed Consent Statement: Not applicable.

Data Availability Statement: The data are not publicly available due to privacy.

Acknowledgments: We thank Yajima for editing the English text of a draft of this manuscript.

Conflicts of Interest: The authors declare no conflict of interest.

References

1. Ge, Y.; Cheng, Z.H.; Si, X.Y.; Ma, W.H.; Tan, L.; Zang, X.P.; Wu, B.; Xu, Z.N.; Wang, N.; Zhou, Z.X.; et al. Transcriptome profiling provides insight into the genes in carotenoid biosynthesis during the mesocarp and seed developmental stages of avocado (*Persea Americana*). *Int. J. Mol. Sci.* **2019**, *20*, 4117. [[CrossRef](#)] [[PubMed](#)]
2. Kuhn, D.N.; Livingstone, D.S., III; Richards, J.H.; Manosalva, P.; Van den Berg, P.; Chambers, A.H. Application of genomic tools to avocado (*Persea americana*) breeding: SNP discovery for genotyping and germplasm characterization. *Sci. Hortic.* **2019**, *246*, 1–11. [[CrossRef](#)]
3. Schaffer, B.; Wolstenholme, B.N.; Whitley, A.W. *The Avocado: Botany, Production and Uses*, 2nd ed.; CPI Group (UK) Ltd.: Croydon, UK, 2012.
4. Ge, Y.; Zhang, T.; Wu, B.; Tan, L.; Ma, F.N.; Zou, M.H.; Chen, H.H.; Pei, J.L.; Liu, Y.Z.; Chen, Z.H.; et al. Genome-wide assessment of avocado germplasm determined from specific length amplified fragment sequencing and transcriptomes: Population structure, genetic diversity, identification, and application of race-specific markers. *Genes* **2019**, *10*, 215. [[CrossRef](#)] [[PubMed](#)]
5. Ge, Y.; Dong, X.S.; Wu, B.; Wang, N.; Chen, D.; Chen, H.H.; Zou, M.H.; Xu, Z.N.; Tan, L.; Zhan, R.L. Evolutionary analysis of six chloroplast genomes from three *Persea americana* ecological races: Insights into sequence divergences and phylogenetic relationships. *PLoS ONE* **2019**, *14*, e0221827. [[CrossRef](#)] [[PubMed](#)]
6. Dreher, M.L.; Davenport, A.J. Hass avocado composition and potential health effects. *Crit. Rev. Food Sci.* **2013**, *53*, 738–750. [[CrossRef](#)]

7. Ge, Y.; Zang, X.P.; Yang, Y.; Wang, T.; Ma, W.H. In-depth analysis of potential PaAP2/ERF transcription factor related to fatty acid accumulation in avocado (*Persea americana* Mill.) and functional characterization of two PaAP2/ERF genes in transgenic tomato. *Plant. Physiol. Biochem.* **2021**, *158*, 308–320. [[CrossRef](#)]
8. Kilaru, A.; Cao, X.; Dabbs, P.B.; Sung, H.J.; Rahman, M.M.; Thrower, N.; Zynda, G.; Podicheti, R.; Ibarra-Laclette, E.; Herrera-Estrella, L.; et al. Oil biosynthesis in a basal angiosperm: Transcriptome analysis of *Persea americana* mesocarp. *BMC Plant. Biol.* **2015**, *15*, 203. [[CrossRef](#)]
9. Ge, Y.; Si, X.Y.; Cao, J.Q.; Zhou, Z.X.; Wang, W.L.; Ma, W.H. Morphological characteristics, nutritional quality, and bioactive constituents in fruits of two avocado (*Persea americana*) varieties from hainan province, China. *J. Agric. Sci.* **2017**, *9*, 8–17. [[CrossRef](#)]
10. Ge, Y.; Ma, F.N.; Wu, B.; Tan, L. Morphological and chemical analysis of 16 avocado accessions (*Persea americana*) from China by principal component analysis and cluster analysis. *J. Agric. Sci.* **2018**, *10*, 80–89. [[CrossRef](#)]
11. Chen, G.L.; Chen, S.G.; Zhao, Y.Y.; Luo, C.X.; Li, J.; Gao, Y.Q. Total phenolic contents of 33 fruits and their antioxidant capacities before and after in vitro digestion. *Ind. Crop. Prod.* **2014**, *57*, 150–157. [[CrossRef](#)]
12. Kosinska, A.; Karamac, M.; Estrella, I.; Hernandez, T.; Bartolome, B.; Dykes, G.A. Phenolic compound profiles and antioxidant capacity of *Persea americana* Mill. peels and seeds of two varieties. *J. Agric. Food Chem.* **2012**, *60*, 4613–4619. [[CrossRef](#)]
13. Vinha, A.F.; Moreira, J.; Barreira, S.V.P. Physicochemical parameters, phytochemical composition and antioxidant activity of the Algarvian avocado (*Persea americana* Mill.). *J. Agric. Sci.* **2013**, *5*, 100–109. [[CrossRef](#)]
14. Weckwerth, W. Metabolomics in systems biology. *Ann. Rev. Plant. Biol.* **2003**, *54*, 669–689. [[CrossRef](#)] [[PubMed](#)]
15. Chen, W.L.; Gong, Z.; Guo, W.S.; Wang, H.Y.; Zhang, X.O.; Liu, S.B.; Yu, L.Z.; Xiong, J. A novel integrated method for large-scale detection, identification, and quantification of widely targeted metabolites: Application in the study of rice metabolomics. *Mol. Plant.* **2013**, *6*, 1769–1780. [[CrossRef](#)]
16. Sawada, Y.; Akiyama, K.; Sakata, A.; Kuwahara, A.; Otsuki, H.; Sakurai, T.; Saito, K.; Hirai, M.Y. Widely targeted metabolomics based on large-scale MS/MS data for elucidating metabolite accumulation patterns in plants. *Plant. Cell Physiol.* **2009**, *50*, 37–47. [[CrossRef](#)]
17. Tan, H.; Zhang, J.; Qi, X.; Shi, X.L.; Zhou, J.G.; Wang, X.C.; Xiang, X.E. Correlation analysis of the transcriptome and metabolome reveals the regulatory network for lipid synthesis in developing *Brassica napus* embryos. *Plant. Mol. Biol.* **2019**, *99*, 31–44. [[CrossRef](#)] [[PubMed](#)]
18. Khan, W.A.; Hou, X.; Han, K.; Khan, N.; Dong, H.; Saqib, M.; Zhang, Z.; Naseri, E.; Hu, C. Lipidomic study reveals the effect of morphological variation and other metabolite interactions on the lipid composition in various cultivars of Bok choy. *Biochem. Biophys. Res. Commun.* **2018**, *506*, 755–764. [[CrossRef](#)]
19. Zhi, Y.; Taylor, M.C.; Campbell, P.M.; Warden, A.C.; Shrestha, P.; El Tahchy, A.; Rolland, V.; Vanhercke, T.; Petrie, J.R.; White, R.G.; et al. Comparative lipidomics and proteomics of lipid droplets in the mesocarp and seed tissues of Chinese tallow (*Triadica sebifera*). *Front. Plant. Sci.* **2017**, *8*, 1339. [[CrossRef](#)]
20. Ge, Y.; Dong, X.S.; Liu, Y.Z.; Yang, Y.; Zhan, R.L. Molecular and biochemical analyses of avocado (*Persea americana*) reveal differences in the oil accumulation pattern between the mesocarp and seed during the fruit developmental period. *Sci. Hortic.* **2021**, *276*, 109717. [[CrossRef](#)]
21. Rendón-Anaya, M.; Ibarra-Laclette, E.; Méndez-Bravo, A.; Lan, T.Y.; Zheng, C.F.; Carretero-Paulet, L.; Perez-Torres, C.A.; Chacón-López, A.; Hernández-Guzmán, G.; Chang, T.H. The avocado genome informs deep angiosperm phylogeny, highlights introgressive hybridization, and reveals pathogen-influenced gene space adaptation. *Proc. Natl. Acad. Sci. USA* **2019**, *116*, 17081–17089. [[CrossRef](#)]
22. Livak, K.J.; Schmittgen, T.D. Analysis of relative gene expression data using real-time quantitative PCR and the $2^{-\Delta\Delta CT}$ method. *Methods* **2001**, *25*, 402–408. [[CrossRef](#)]
23. Walther, T.C.; Chung, J.Y.; Farese, R.V., Jr. Lipid droplet biogenesis. *Annu. Rev. Cell Dev. Bi.* **2017**, *33*, 491–510. [[CrossRef](#)] [[PubMed](#)]
24. Yang, Z.L.; Ji, H.Y.; Liu, D.T. Oil biosynthesis in underground oil-rich storage vegetative tissue: Comparison of *Cyperus esculentus* ruber with oil seeds and fruits. *Plant. Cell Physiol.* **2016**, *57*, 2519–2540. [[CrossRef](#)]
25. Gidda, S.K.; Watt, S.; Collins-Silva, J.; Kilaru, A.; Arondel, V.; Yurchenko, O.; Horn, P.J.; James, C.N.; Shintani, D.; Ohlrogge, J.B. Lipid droplet-associated proteins (LDAPs) are involved in the compartmentalization of lipophilic compounds in plant cells. *Plant. Signal. Behav.* **2013**, *8*, e27141. [[CrossRef](#)] [[PubMed](#)]
26. Horn, P.J.; James, C.N.; Gidda, S.K.; Kilaru, A.; Dyer, J.M.; Mullen, R.T.; Ohlrogge, J.B.; Chapman, K.D. Identification of a new class of lipid droplet-associated proteins in plants. *Plant. Physiol.* **2013**, *162*, 1926–1936. [[CrossRef](#)] [[PubMed](#)]
27. Gross-German, E.; Viruel, M.A. Molecular characterization of avocado germplasm with a new set of SSR and EST-SSR markers: Genetic diversity, population structure, and identification of race-specific markers in a group of cultivated genotypes. *Tree Genet. Genomes* **2013**, *9*, 539–555. [[CrossRef](#)]
28. Ashworth, V.E.T.M.; Clegg, M.T. Microsatellite markers in avocado (*Persea americana* Mill.). genealogical relationships among cultivated avocado genotypes. *J. Hered.* **2003**, *94*, 407–415. [[CrossRef](#)]

-
29. Schnell, R.J.; Brown, J.S.; Olano, C.T.; Power, E.J.; Krol, C.A.; Kuhn, D.N.; Motamayor, J.C. Evaluation of avocado germplasm using microsatellite markers. *J. Amer. Soc. Hort. Sci.* **2003**, *128*, 881–889. [[CrossRef](#)]
 30. Lu, S.P.; Sturtevant, D.; Aziz, M.; Jin, C.; Li, Q.; Chapman, K.D.; Guo, L. Spatial analysis of lipid metabolites and expressed genes reveals tissue-specific heterogeneity of lipid metabolism in high- and low-oil *Brassica napus* L. seeds. *Plant. J.* **2018**, *94*, 915–932. [[CrossRef](#)]